

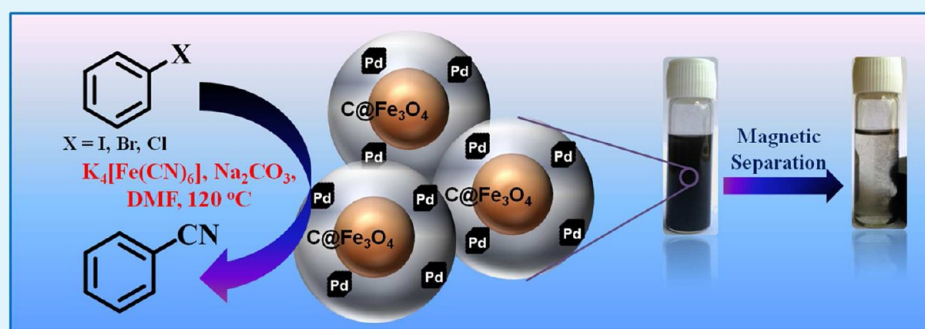
Fabrication of Pd Nanoparticles Embedded C@Fe₃O₄ Core–Shell Hybrid Nanospheres: An Efficient Catalyst for Cyanation in Aryl Halides

Basuvaraj Suresh Kumar,[†] Arlin Jose Amali,^{*,†,‡} and Kasi Pitchumani^{*,†,‡}

[†]Department of Natural Products Chemistry, School of Chemistry, Madurai Kamaraj University, Madurai 625 021, Tamilnadu, India

[‡]Centre for Green Chemistry Processes, School of Chemistry, Madurai Kamaraj University, Madurai 625 021, Tamilnadu, India

S Supporting Information



ABSTRACT: Isolated chemical reactors were fabricated by integrating catalytically active sites (Pd) with magnetic functionality (Fe₃O₄) along with carbon while preserving the constituents functional properties to realize the structure–property relationship of Pd by comparing the catalytic activity of spherical Pd NPs with cubical Pd NPs for cyanation in aryl halides using K₄[Fe(CN)₆] as a green cyanating agent to yield corresponding nitriles. The superior catalytic reactivity of the cubical Pd NPs is attributed to the larger number of {100} surface facets. The TEM images of reused catalyst shows the change in structure from cubical to spherical nanoparticles, attributed to the efficient leaching susceptibility of Pd {100} surface facets. The cubical Pd NPs on carbon@Fe₃O₄ is attractive in view of its high catalytic efficiency, easy synthesis, magnetic separability, environmental friendliness, high stability, gram scale applicability, and reusability.

KEYWORDS: shape sensitivity, palladium nanocubes, palladium nanoparticles, carbon@Fe₃O₄, K₄[Fe(CN)₆], {100} surface facets

INTRODUCTION

Noble metal nanomaterials receive considerable attention due to their excellent optical,¹ catalytic,² and photothermal³ properties which have resulted in exciting applications in nanocatalysis,⁴ nanosensing,⁵ and drug delivery.⁶ Nanocatalysis is an emerging frontier in catalysis, where in the catalytic activity strongly depends on the nanoparticle size,⁷ its shape, and the number of surface (vertex, edge, and plane) atoms which are important parameters that contribute profoundly to the active catalytic sites. Recently, considerable attention has been given to the design and manipulation of well-defined structures with a specific facet exposure,^{8,9} which provides a critical way to finely tune the physicochemical properties and thus rationally optimize their reactivity and selectivity. As such, surface structure control is of special significance to the heterogeneous catalysis, because a heterogeneous catalytic reaction involves many surface-related steps, such as adsorption and activation of reactants on specific surface sites, chemical transformation of adsorbed species, and desorption of products.^{10,11}

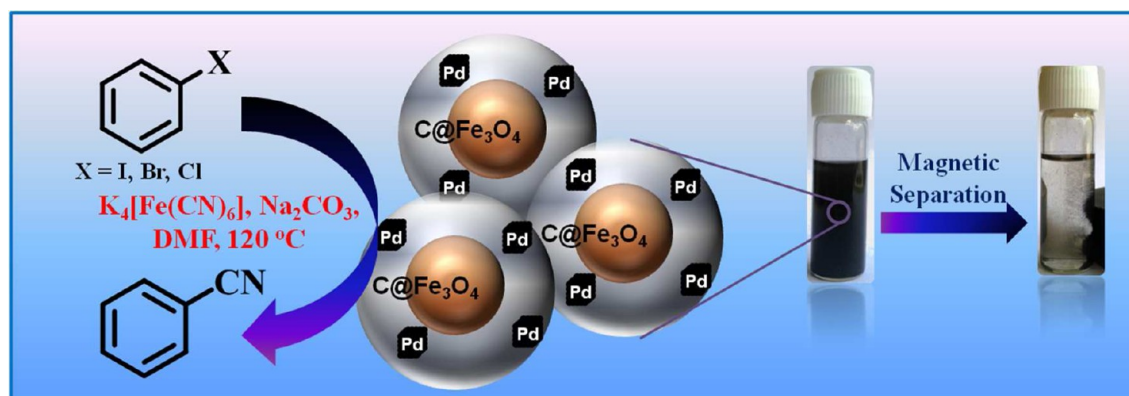
Palladium (Pd) is among the most widely used transition metals in modern organic synthesis.^{12,13} Development of high-performance Pd nanoparticles (Pd NPs) catalysts by the strategy of controlling the particle shape can be an effective way to improve the catalytic activity on a mass basis. By taking into account both size and surface structures, one can tailor the catalytic activity of a Pd-based catalyst at the nanoscale by controlling the shape of Pd NPs during their chemical syntheses. The performance of Pd NPs in various heterogeneous catalytic processes have been found to be highly dependent on the exposed facets,¹⁴ which determines the arrangement and coordination of the surface atoms.

Arylnitriles represent an integral part in dyes, herbicides, agrochemicals, pharmaceuticals, and natural products.¹⁵ The classical synthesis of aromatic nitriles by the Sandmeyer and Rosenmund–von Braun reactions^{16,17} are associated with serious drawbacks, such as stoichiometric amounts of highly

Received: June 28, 2015

Accepted: September 29, 2015

Published: September 29, 2015

Scheme 1. Schematic Representation for Cyanation of Aryl Halides Using Pd NCs/C@Fe₃O₄ Nanospheres

toxic copper(I) cyanide as the cyanating agent, which leads to equimolar amounts of heavy metal waste and high temperature. In the past, the cyanide sources involved in cyanation of aryl halides are primarily toxic alkali metal cyanides such as KCN, NaCN,^{18–20} Zn(CN)₂,²¹ CuCN,²² and TMSCN²³ as well as relatively less toxic alternative cyanide sources such as alkyl nitriles,²⁴ acetone cyanohydrins,²⁵ phenyl cyanate.²⁶ Although Pd catalysts are highly efficient in cyanation reaction,²⁷ a general problem of these Pd catalyzed cyanations is the high affinity of cyanide toward Pd and often a fast deactivation of the catalytic system is observed due to the formation of stable cyanide complexes and consequently catalysis proceeds with low efficiency, which significantly inhibits the catalytic cycle. Beller and co-workers^{28,29} have used a relatively nontoxic and inexpensive K₄[Fe(CN)₆] as a cyanide source in cyanation reactions. The significant advantages of this reagent are (a) involvement of all the six CN⁻ ions of K₄[Fe(CN)₆] in cyanation of aryl halides and this harnesses the full potential of the reagent and (b) the cyanide ion is strongly bound in potassium ferrocyanide(II), warranting substantially slow release of cyanide ions which may be beneficial for reducing the inactivation of the catalyst. Since then a number of reports were available using this reagent in the presence of Pd catalysts such as Pd(OAc)₂,^{30,31} several Pd complexes^{32–45} and Pd/C^{46,47} were developed. The serious drawbacks of these metal catalysts are metal contaminations in the final products, nonreusability, and deactivation of the catalysts associated with the use of the homogeneous system and hence are still unwelcoming. Recycling of the catalysts is a task of great practical, economic, and environmental importance. Thus, a more efficient and convenient protocol for this important transformation would be appreciated, and hence in recent years, considerable attention has been paid to the development of Pd NPs with improved catalytic properties in cyanation reactions.^{48–53}

The most common problems associated with nanocatalysts are tedious filtration and centrifugation protocols. Additionally NPs undergo agglomeration without the addition of stabilizers, thereby diminishing their activity. To circumvent this, there have been many efforts to stabilize the NPs by immobilization on different supports, such as charcoal, silica, or alumina.^{54–56} However, though this may result in high catalytic activities, the stability toward metal leaching is not satisfactory.⁵⁷ Alternatively, encapsulation of the metal NPs on polymers^{58–60} have been reported, but the catalysts further require mechanical stability against breakage of the host or leaching of the metallic

particles. Also, many of these supports have limitations including the difficulty in their synthesis, their tiresome recovery using centrifugation, or time-consuming filtration. A superb way of combining high surface area of nanocatalysts along with ease in recovery involve use of an external magnet via magnetic support for catalytic applications.^{61–63} Incorporation of the magnetic support (e.g., Fe₃O₄) also provides an additional functionality to the catalyst system for easy separation from the reaction medium by using an external magnetic field. Consequently many efforts were made to fabricate Fe₃O₄-based magnetic nanocatalysts. Among them, carbonaceous materials as the shells have aroused much interest because of their outstanding intrinsic properties, such as large surface area, acid and base resistance, highly thermal stability (inert gas atmosphere), and abundant functional groups.

Herein, we developed for the first time, the shape-dependency in catalytic activity of Pd NPs were probed by comparing the catalytic activity of spherical Pd NPs with cubical Pd NPs on C@Fe₃O₄ in cyanation reaction using K₄[Fe(CN)₆] as a green cyanating agent (Scheme 1). The main advantage of this catalyst is heterogeneous, structurally stable catalytic sites which makes them recyclable without any loss in activity, easy recovery by applying an external magnet, ligand free methodology.

EXPERIMENTAL SECTION

Chemicals. Sodium tetrachloropalladate (Na₂PdCl₄), polyvinylpyrrolidone (PVP), potassium bromide (KBr), ascorbic acid (AA), potassium phosphate tribasic (K₃PO₄), 4-iodoacetophenone (98%), 1-iodo-3,4-dimethylbenzene (99%), 4-iodoaniline (98%), 4-iodophenol (99%), 3-iodobenzotrifluoride (98%), 4-iodoanisole (99%), 4-iodonitrobenzene (98%), 4-bromobenzotrifluoride (99%), 2-bromo-5-methylpyridine (99%), 2-bromonaphthalene (99%), 4-bromochlorobenzene (98%), 4-bromopyridine (98%), and 4-chlorobenzaldehyde (97%) were obtained from Sigma-Aldrich and used as received. Bromobenzene (98%), chlorobenzene (99%), potassium chloride (KCl), potassium carbonate (K₂CO₃), D(+)-glucose, iron(III)chloride hexahydrate, urea, ethylene glycol, water HPLC grade, dimethylformamide (DMF), dimethyl sulfoxide (DMSO), ethyl acetate, and toluene were obtained from Merck. Potassium ferrocyanide(II) (K₄[Fe(CN)₆]·3H₂O), potassium iodide (KI) were obtained from Qualigens Fine Chemicals and used as received. Sodium carbonate (Na₂CO₃), triethylamine (TEA), and sodium sulfate (Na₂SO₄) were obtained from Hi-Media. Cesium carbonate (Cs₂CO₃) and 4-bromobenzaldehyde (98%) were obtained from Avra Synthesis. 4-Bromobenzonitrile (98%) and 4-bromotoluene (99%) were obtained from Alfa Aesar. 4-Chloroacetophenone (98%) was obtained from SD-Fine Chemicals. 3-Nitrochlorobenzene (98%) was obtained from Sisco Chemicals.

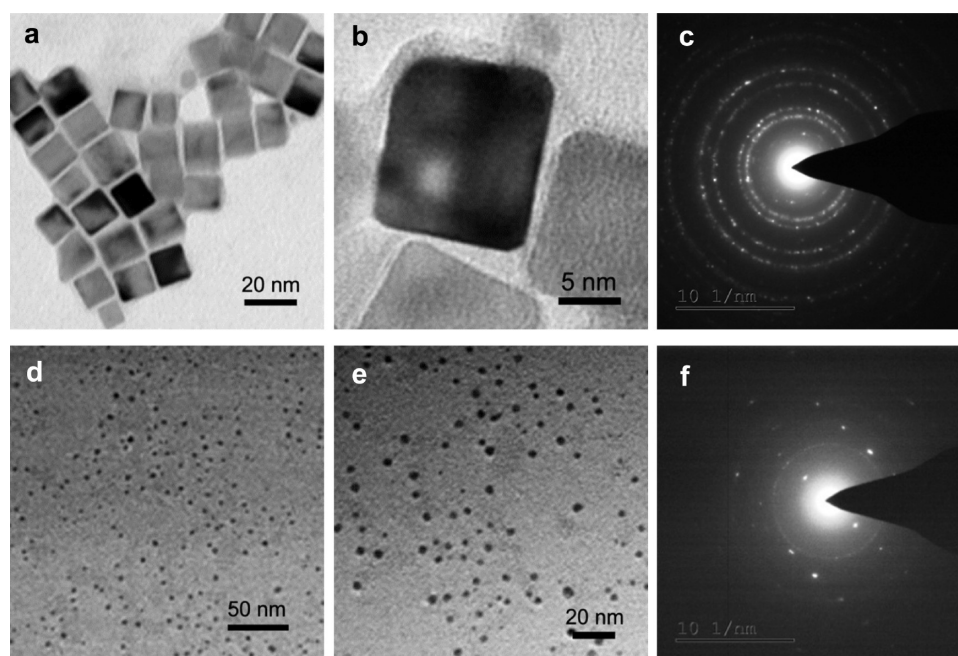


Figure 1. TEM images of (a, b) Pd NCs, (d, e) Pd NPs, and SAED patterns of (c) Pd NCs and (f) Pd NPs.

Synthesis of Pd Nanocubes (Pd NCs). The Pd NCs were synthesized by adding an aqueous solution of Na_2PdCl_4 into an aqueous solution of PVP, AA, KBr, and KCl in accordance with a previously reported method.⁶⁴ In a typical procedure, an aqueous solution (8.0 mL) containing PVP (105 mg), AA (60 mg), KBr (600 mg), and KCl (185 mg) was placed in a vial and preheated to 80 °C in an oil bath under magnetic stirring for 10 min. Subsequently, an aqueous solution (3.0 mL) containing Na_2PdCl_4 (57 mg) was added with a pipet. The reaction was allowed to continue at 80 °C for 3 h to afford Pd NCs. The Pd NCs were collected by centrifugation (3000 rpm, 20 min). The collected Pd NCs were washed several times with water to remove excess PVP and redispersed in water (11.0 mL).

Synthesis of Pd Nanoparticles (Pd NPs). The Pd NPs were synthesized by adding an aqueous solution of Na_2PdCl_4 into an aqueous solution of PVP and AA in accordance with a reported method with slight modification.⁶⁵ In a typical procedure, an aqueous solution (8.0 mL) containing PVP (105 mg) and AA (60 mg) was placed in a vial and preheated to 80 °C in an oil bath under magnetic stirring for 10 min. Subsequently, an aqueous solution (3.0 mL) containing Na_2PdCl_4 (57 mg) was added with a pipet. The reaction was allowed to continue at 80 °C for 3 h to obtain Pd NPs and the Pd NPs were separated from the reaction mixture by centrifugation (4000 rpm, 20 min). The collected Pd NPs were washed several times with water to remove excess PVP and redispersed in water (11.0 mL).

Hydrothermal Synthesis of Fe_3O_4 Nanospheres (Fe_3O_4 NSs). Fe_3O_4 NSs were synthesized by modification of a previously reported method.⁶⁶ Typically, iron(III) chloride hexahydrate (1 mmol, 0.270 g) and urea (9 mmol, 0.540 g) were added into ethylene glycol (10 mL) under magnetic stirring. The resultant solution was transferred into a Teflon lined stainless steel autoclave, sealed, and heated to 200 °C for 12 h. The precipitated black products were collected by an external magnet and washed several times with ethanol. Finally, the black colored product was dried in vacuum for 24 h at 60 °C.

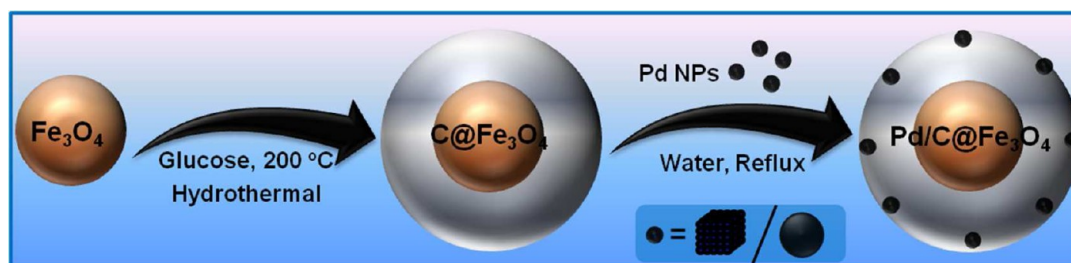
Fabrication of Carbon@ Fe_3O_4 Nanospheres ($\text{C}@Fe_3O_4$). Carbon@ Fe_3O_4 were synthesized by *in situ* carbonization of glucose in the presence of Fe_3O_4 under hydrothermal conditions.⁶⁷ The synthesized Fe_3O_4 solid spheres (100 mg) were dispersed in water (10 mL) containing glucose (1.6 g) by ultrasonication. It was transferred into a Teflon lined stainless steel autoclave, sealed, and heated at 160 °C for 10 h and cooled down at room temperature. The precipitated black solid was collected from the solution by an external magnet and washed several times with ethanol followed by water. Finally, the black

colored product was obtained. This was dried in vacuum for 24 h at 60 °C to afford $\text{C}@Fe_3O_4$.

Incorporation of Pd NCs and Pd NPs in Carbon@ Fe_3O_4 ($\text{Pd}/\text{C}@Fe_3O_4$). $\text{Pd}/\text{C}@Fe_3O_4$ was prepared by deposition method. Typically, carbon@ Fe_3O_4 (400 mg) was well dispersed in ethylene glycol (40 mL) under magnetic stirring. To this Pd NCs/Pd NPs solutions were added dropwise for 30 min under vigorous stirring. The above prepared solution was stirred at 2 h, under 60 °C conditions. After completion of the reaction, the Pd NCs/Pd NPs incorporated $\text{C}@Fe_3O_4$ were separated by an external magnet and washed several times with water. The products were dried in vacuum to obtain $\text{Pd}/\text{C}@Fe_3O_4$.

Characterization. The powder X-ray diffraction (PXRD) analysis was carried out on a Seimens (Cheshire, U.K.) D5000 X-ray diffractometer using $\text{CuK}\alpha$ ($\lambda = 1.5406 \text{ \AA}$) radiation at 40 kV and 30 mA with a standard monochromator using a Ni filter with a scanning angle (2θ) of 10°–70°. High-resolution transmission electron microscope (HRTEM) characterization was carried out with a Tecnai G² Spirit microscope operating at 200 kV. The ultraviolet-diffuse reflectance spectra (UV-DRS) were recorded in Jasco V 550 instrument with the wavelength range between 200–600 nm. FT-IR spectra were recorded in Thermo Scientific Nicolet iS50 FT-IR spectrometer using a KBr wafer with wavenumber ranging 4000–400 cm^{-1} . The morphology of the synthesized materials was analyzed in a VEGA 3 LM analytical scanning electron microscope (SEM). The metal loadings of the catalysts were determined by SEM with energy dispersive X-ray analysis (EDX) on a Bruker-nano instrument. ICP-OES analyses were performed in PerkinElmer Optima 5300 DV ICP-OES instrument. Gas chromatography analyses were performed on a Shimadzu GC-17A system. NMR spectra were recorded in Bruker 300 MHz instrument with tetramethylsilane as an internal standard and CDCl_3 as solvent.

$\text{Pd}/\text{C}@Fe_3O_4$ Catalyzed Cyanation of Aryl Halides. $\text{K}_4[\text{Fe}(\text{CN})_6]\cdot 3\text{H}_2\text{O}$ was ground to a fine powder and dried in vacuum at 80 °C overnight. In a typical reaction procedure for aryl iodides (0.5 mmol), dry $\text{K}_4[\text{Fe}(\text{CN})_6]$ (0.1 mmol), Na_2CO_3 (0.2 mmol), 20 mg of $\text{Pd}/\text{C}@Fe_3O_4$ (0.73 mol % of Pd), DMF (3 mL), and KI for aryl bromides and aryl chlorides as substrates (0.2 mmol) are taken in a Schlenk tube with a Teflon stopcock, sealed, and heated at 120 °C with magnetic stirring. The progress of the reaction was monitored by TLC, after progression of the reaction, the mixture was cooled to room temperature and the catalyst was separated by applying an

Scheme 2. Schematic Illustration Mechanism for Formation of Pd/C@Fe₃O₄ Nanospheres

external magnet. After removal of catalyst water was added to the solution and extracted with ethyl acetate. The organic phase is dried over anhydrous Na₂SO₄. After evaporation of the solvents, the residue is subjected to GC analysis, which was further purified by column chromatography over silica gel (60–120 mesh) eluting with pet ether/ethyl acetate (90:10) to afford the desired nitrile product. The nitrile products were confirmed by the spectroscopic method using ¹H and ¹³C NMR (Figure S8a–n in the Supporting Information). This procedure was followed for all of the reactions listed in Table 2.

RESULTS AND DISCUSSION

The Pd NCs are prepared using a water-based process that involves injection of Pd²⁺ into an aqueous solution of AA at 80 °C, with Br[−] and Cl[−] ions serving as capping agents and PVP acting as a stabilizer.⁶⁴ Besides capping the {100} facets of Pd NCs, the halide species decrease the rate of reduction of the Pd²⁺ ions. TEM images of the Pd NCs indicate a cubic structure with an edge length of 13 nm and surfaces covered by {100} facets (Figure 1a,b). The Pd NCs are found to be highly crystalline as indicated from the SAED pattern (Figure 1c). Pd NPs were prepared by the reduction of Na₂PdCl₄ with AA in the aqueous solution of PVP. AA reduces the Pd²⁺ ions to give Pd NPs, which are stabilized and prevented from agglomeration by PVP. TEM images reveal that well-dispersed Pd NPs with particle sizes of 3–4 nm are obtained (Figure 1d,e). The corresponding SAED pattern indicates that the Pd NPs are crystalline (Figure 1f).

A three step procedure was used to fabricate the Pd incorporated carbon@Fe₃O₄ nanospheres to study the structure–property relationship of Pd in cyanation reactions (Scheme 2). Ferrite NPs were synthesized using a robust hydrothermal reaction based on high-temperature reduction of Fe(III) ions with ethylene glycol serving both as a solvent and a reducing agent and urea as the capping agent. Second, a thin layer of carbon shells have been coated on the surface of the ferrite NPs through the carbonization of glucose under hydrothermal conditions. The thin layer of carbon shell has two functions: (a) it can protect the magnetic particles from being corrupted and oxidized by acids and oxygen; and (b) the presence of functional groups such as –COOH, –OH, and –C=O can be beneficially used to immobilize a catalytic active species.⁶⁸ Finally, the presynthesized Pd NPs/NCs were immobilized on the carbon shell by refluxing. The final morphology of the hybrid nanospheres shows a core–shell feature (C@Fe₃O₄) with fine particles of Pd deposited on the surface, resulting in a nanocomposite.

FE-SEM analysis of the synthesized nanocomposite clearly illustrates spherical morphology of Fe₃O₄ with particle sizes of 100–150 nm (Figure 2a). Further analysis by TEM reveals the porous nature of the Fe₃O₄ NPs (Figure 2b,c). Following the carbonization of glucose on Fe₃O₄ NPs, it is clearly observed that the prepared C@Fe₃O₄ nanospheres remain spherical and

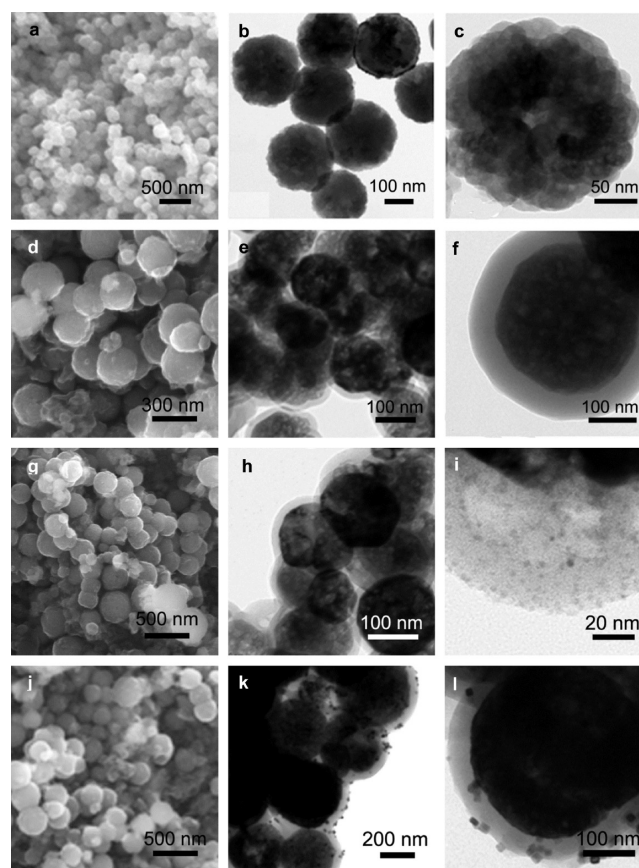


Figure 2. FE-SEM images of (a) Fe₃O₄, (d) C@Fe₃O₄, (g) Pd NPs/C@Fe₃O₄, and (j) Pd NCs/C@Fe₃O₄ and TEM images of (b,c) Fe₃O₄, (e,f) C@Fe₃O₄, (h,i) Pd NPs/C@Fe₃O₄, and (k,l) Pd NCs/C@Fe₃O₄.

consist of a Fe₃O₄ core with carbon-shell (Figure 2d–f). The particle size is 120–150 nm, the thickness of the carbon shell formed from the carbonization of glucose is about 20–25 nm. TEM images clearly reveal the firmly immobilized Pd NPs/Pd NCs on the surface of C@Fe₃O₄ nanospheres (Figure 2h,i and k,l). It is also noticed that none of the Pd NPs/Pd NCs are free and all of them are attached on the C@Fe₃O₄ nanospheres.

The crystallinity and phase composition of the resulting products were further investigated by powder X-ray powder diffraction (PXRD). The PXRD pattern (Figure 3a) (i) confirms that the nanoparticles are magnetite (Fe₃O₄) and the average crystallite size, estimated using Scherrer's equation, is 101 nm. The crystallite size matches with the average particle size (100–110 nm) seen in the TEM analysis indicating that the particles are constituted of a single crystalline domain. Further, PXRD patterns (Figure 3a) (iii,iv) show that Pd forms

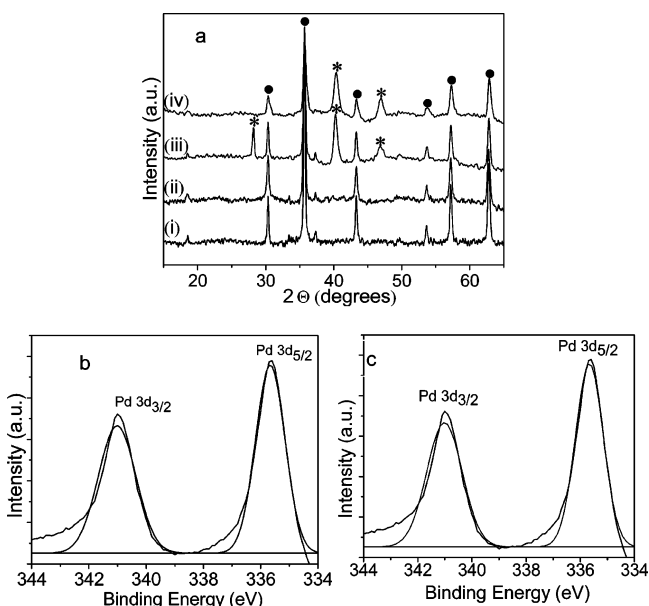


Figure 3. (a) X-ray powder diffraction patterns of (i) Fe_3O_4 , (ii) $\text{C}@ \text{Fe}_3\text{O}_4$, (iii) Pd NCs/ $\text{C}@ \text{Fe}_3\text{O}_4$, and (iv) Pd NPs/ $\text{C}@ \text{Fe}_3\text{O}_4$. The \bullet stands for Fe_3O_4 and * stands for Pd, and XPS spectra of (b) Pd NCs/ $\text{C}@ \text{Fe}_3\text{O}_4$ and (c) Pd NPs/ $\text{C}@ \text{Fe}_3\text{O}_4$ show Pd $3d_{5/2}$ and Pd $3d_{3/2}$ binding energies.

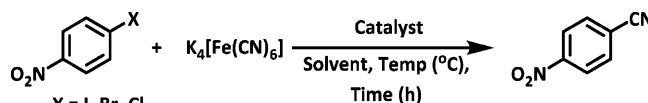
a face centered cubic (fcc) structure. For Pd, the diffraction peaks are observed at 2θ values 28.18° , 40.27° , 46.88° , and 68.33° , which can be attributed to (100), (111), (200), and (220) planes, respectively. The intensity ratio of (111) to (200) peaks in Pd NPs is significantly lower than the Pd NCs (from 3.90 to 2.17), which indicates that the (100) planes dominate in the Pd NCs.⁶⁹

The UV-DRS spectrum of Fe_3O_4 displays a broad absorption range, of 450 to 600 nm, indicating that iron is present in the form of Fe_3O_4 (Figure S1a).⁷⁰ The red shift in absorbance of the $\text{C}@ \text{Fe}_3\text{O}_4$ nanospheres may be attributed to the formation of the carbon shell on Fe_3O_4 nanospheres (Figure S1b). The FT-IR spectrum of Fe_3O_4 shows that the stretching frequency at 581 cm^{-1} , is assigned to be Fe–O (Figure S2a). The peaks at $1600\text{--}1700$ and 3400 cm^{-1} indicate the existence of hydrophilic carboxyl groups on the surface of the $\text{C}@ \text{Fe}_3\text{O}_4$ nanospheres (Figure S2b). The TGA analysis reveals a small weight loss from room temperature to $150\text{ }^\circ\text{C}$ due to dehydration followed by a weight loss from 300 to $450\text{ }^\circ\text{C}$ due to the combustion of the carbon. From the weight loss, the carbon content was calculated to be 73 wt % and the balance (27 wt %) was assumed to be Fe_3O_4 (Figure S3a,b).

The energy-dispersive X-ray spectroscopic (EDX) point analyses of randomly chosen Pd NCs/ $\text{C}@ \text{Fe}_3\text{O}_4$ and Pd NPs/ $\text{C}@ \text{Fe}_3\text{O}_4$ display uniform compositions (Figures S4 and S5). The analyses reveal the elemental composition of palladium as 1.58 wt % for Pd NCs and 1.50 wt % for Pd NPs on $\text{C}@ \text{Fe}_3\text{O}_4$. This result clearly suggests that all the Pd NPs were uniformly deposited on the surface of $\text{C}@ \text{Fe}_3\text{O}_4$ nanospheres. Inductively coupled plasma-optical emission spectrometric (ICP-OES) analyses showed that the Pd/ $\text{C}@ \text{Fe}_3\text{O}_4$ contain 3.6×10^{-6} mol for Pd NCs and 3.1×10^{-6} mol for Pd NPs on $\text{C}@ \text{Fe}_3\text{O}_4$. The oxidation state of Pd was ascertained by X-ray photoelectron spectroscopy (XPS). The binding energy of 335.5 eV could be attributed to the Pd $3d_{5/2}$ level of Pd(0) (Figure 3b,c).⁷¹

The catalytic performance of the Pd NCs/ $\text{C}@ \text{Fe}_3\text{O}_4$ catalyst was evaluated in the cyanation reaction of aryl iodides, bromides, and chlorides with $\text{K}_4[\text{Fe}(\text{CN})_6]$ as a green cyanating agent. To optimize the reaction conditions, control experiments were performed with a representative reaction of 4-nitroiodobenzene and $\text{K}_4[\text{Fe}(\text{CN})_6]$ with base, solvent, catalyst loading, temperature, and time are the important parameters. Initially the reaction failed without Pd, thus clearly suggesting the active role of Pd-center in this reaction. With cubical Pd NPs/ $\text{C}@ \text{Fe}_3\text{O}_4$, the corresponding nitrile product was formed in 99% yield (Table 1, entries 1–3). Without base the reaction

Table 1. Optimization of Reaction Conditions in the Cyanation of 4-Iodonitrobenzene^a



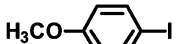
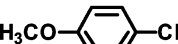
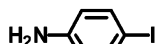
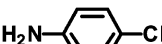
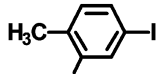
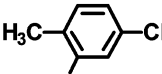
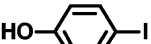

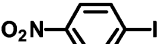
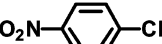
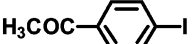
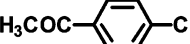
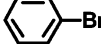
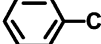
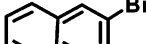
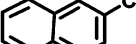


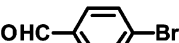
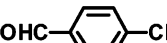

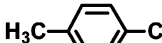
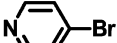
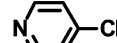

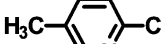


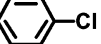
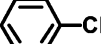

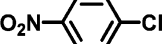
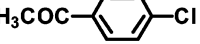
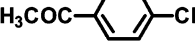
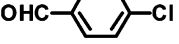
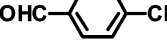

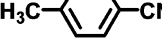
entry	catalyst	base	solvent	time (h)	conversion ^b (%)
1	Fe_3O_4	K_2CO_3	DMF	24	Nil
2	$\text{Fe}_3\text{O}_4@ \text{C}$	K_2CO_3	DMF	24	Nil
3	Pd NCs/ $\text{C}@ \text{Fe}_3\text{O}_4$	K_2CO_3	DMF	18	>99
4	Pd NCs/ $\text{C}@ \text{Fe}_3\text{O}_4$		DMF	18	Nil
5	Pd NCs/ $\text{C}@ \text{Fe}_3\text{O}_4$	$\text{K}_3(\text{PO}_4)_2$	DMF	18	8
6	Pd NCs/ $\text{C}@ \text{Fe}_3\text{O}_4$	Na_2CO_3	DMF	18	> 99
7	Pd NCs/ $\text{C}@ \text{Fe}_3\text{O}_4$	Cs_2CO_3	DMF	18	> 99
8	Pd NCs/ $\text{C}@ \text{Fe}_3\text{O}_4$	TEA	DMF	18	45
9	Pd NCs/ $\text{C}@ \text{Fe}_3\text{O}_4$	Na_2CO_3	DMSO	18	75
10	Pd NCs/ $\text{C}@ \text{Fe}_3\text{O}_4$	Na_2CO_3	toluene	18	Nil
11	Pd NCs/ $\text{C}@ \text{Fe}_3\text{O}_4$	Na_2CO_3	DMSO/ H_2O	18	55
12	Pd NCs/ $\text{C}@ \text{Fe}_3\text{O}_4$	Na_2CO_3	DMF	12	99
13	Pd NCs/ $\text{C}@ \text{Fe}_3\text{O}_4$	Na_2CO_3	DMF	10	99
14	Pd NCs/ $\text{C}@ \text{Fe}_3\text{O}_4$	Na_2CO_3	DMF	7	70
15	Pd NCs/ $\text{C}@ \text{Fe}_3\text{O}_4$	Na_2CO_3	DMF	10	>99 ^c
16	Pd NCs/ $\text{C}@ \text{Fe}_3\text{O}_4$	Na_2CO_3	DMF	10	69 ^d
17	Pd NCs/ $\text{C}@ \text{Fe}_3\text{O}_4$	Na_2CO_3	DMF	10	Nil ^e
18	Pd NCs/ $\text{C}@ \text{Fe}_3\text{O}_4$	Na_2CO_3	DMF	10	70 ^f
19	Pd NCs/ $\text{C}@ \text{Fe}_3\text{O}_4$	Na_2CO_3	DMF	10	45 ^g
20	Pd NCs/ $\text{C}@ \text{Fe}_3\text{O}_4$	Na_2CO_3	DMF	32	25 ^h
21	Pd NCs/ $\text{C}@ \text{Fe}_3\text{O}_4$	Na_2CO_3	DMF	18	99 ⁱ

^aReaction conditions: 4-iodonitrobenzene, 0.5 mmol; $\text{K}_4[\text{Fe}(\text{CN})_6]$, 0.1 mmol; catalyst, 20 mg, 0.73 mol % of Pd; solvent, 3 mL; temperature, $120\text{ }^\circ\text{C}$; entries 1–14, 0.5 mmol base. ^bGC yield. ^c0.2 mmol of base. ^d0.1 mmol of Na_2CO_3 . ^eReaction at $80\text{ }^\circ\text{C}$. ^f15 mg (0.54 mol % of Pd) catalyst. ^g10 mg (0.36 mol % of Pd) catalyst. ^hReaction in 4-bromonitrobenzene without KI. ⁱReactions in 4-bromonitrobenzene with KI.

Table 2. Cyanation Reaction of Substituted Aryl Halides in the Presence of Pd NCs/C@Fe₃O₄^a

$$\text{R-X} + \text{K}_4[\text{Fe}(\text{CN})_6] \xrightarrow[\text{DMF, 120 }^\circ\text{C, 10-18 h}]{\text{Pd NCs/C@Fe}_3\text{O}_4} \text{R-CN}$$

X = I, Br, Cl
R = Aryl, heteroaryl

Entry	R-X	Product	Time (h)	Conversion ^b (%)	TON
1			10	96	131
2			10	93	127
3			10	94	128
4			10	94	128
5			10	99	135
6			10	98	134
7			18	99	135
8			18	99	135
9			18	96	131
10			18	99	135
11			10	96	131
12			18	82	112
13			18	77	105
14			18	74	101
15			32	23	16
16			32	30	20
17			32	25	17
18			32	23	16
19			32	20	14

^aReaction conditions: substrate (0.5 mmol), K₄[Fe(CN)₆] = (0.1 mmol); base (0.2 mmol); DMF (3 mL); additive (KI) (0.2 mmol) for bromo and chloro derivatives; temperature, 120 °C; catalyst 20 mg (0.73 mol % of Pd) for I-, Br- and 50 mg (1.8 mol % of Pd) for Cl. ^bGC yield.

failed to proceed (Table 1, entry 4), indicating clearly that cyanation of aryl halides with K₄[Fe(CN)₆] is highly sensitive with respect to the amount and type of base involved in the reaction. The main function of the base is pushing out the

cyanide ion from K₄[Fe(CN)₆]⁷² and it is also involved in the formation of the reactive intermediate.⁷³ Among the various bases tested for this reaction, carbonate bases gave excellent yields (Table 1, entries 3, 6, and 7) compared to other bases,

and this prompted us to choose Na_2CO_3 as the base for this conversion. Among the various solvents used, the reaction works well when polar solvents such as DMF and DMSO were employed (entries 6 and 9, Table 1). In contrast, no product formation is observed in toluene.

The reaction temperature also has a very strong influence on the yield of the reaction. At 80 °C, there is no product (Table 1, entry 17). As the temperature is increased to 120 °C, conversion is increased. It is very difficult to remove the cyanide ion from $\text{K}_4[\text{Fe}(\text{CN})_6]$ under mild reaction conditions due to the high stability/low dissociation of the ferrocyanide ion, covalent bonding behavior of Fe and cyanide ions, and the low solubility of the 4-fold charged anion in organic solvents.²⁷ Hence, the reaction needs high temperature (>100 °C) to release cyanide ion from $\text{K}_4[\text{Fe}(\text{CN})_6]$ and long reaction time (based on size effect of the halides present in the sp^2 carbon) to remove the halide ion in cyanation in aryl halides. While optimizing the catalyst loading, 20 mg (0.73 mol %) of catalyst worked better compared to 15 mg (0.54 mol %) and 10 mg (0.36 mol %) of catalyst (Table 1, entries 18 and 19). On the basis of these observations, the optimum conditions for this Pd catalyzed cyanation of 4-nitroiodobenzene is Pd NCs/C@ Fe_3O_4 (20 mg) as a catalyst in DMF (3 mL) at 120 °C with 0.2 mmol of base for 10 h.

The optimized reaction conditions for cyanation of 4-nitroiodobenzene were extended to the cyanation of 4-bromonitrobenzene and the corresponding nitrile was observed in only 25% yield even after 32 h. The bond dissociation energy of $-\text{C}-\text{X}$ ($\text{X} = \text{I}, \text{Br}, \text{Cl}$) is higher in aryl bromides when compared to aryl iodides. So, the oxidative addition of Pd on aryl bromide is difficult when compare to aryl iodide. Hence, low yield is obtained for aryl bromides in cyanation. Although the result is less satisfactory, we were able to obtain good yield by using iodide ion, which leads to catalyzed production of aryl iodide from aryl bromide and its subsequent *in situ* cyanation, as reported by Buchwald et al.,⁷⁴ and 0.2 mmol of KI is sufficient to promote the cyanation of aryl bromides.

A wide variety of diversely substituted aryl halides underwent cyanation by this procedure to produce the corresponding nitriles (Table 2). Both electron donating [4-OCH₃, 4-NH₂, 4-OH, 3,4-diCH₃] (Table 2, entries 1–4) and electron withdrawing [4-NO₂, 4-COCH₃] (Table 2, entries 5 and 6) substituted aryl iodides reacted readily. However, yields from the aryl iodides substituted with electron withdrawing groups were slightly higher compared to electron donating group substituted aryl iodides. meta-Substituted compounds show slightly lower yield when compared to para-substituted compounds. Similar results were also observed in substituted aryl bromides. Here also aryl bromides substituted with electron withdrawing [4-CN, 4-CHO] (Table 2, entries 9 and 10) groups give higher yields. Significantly, heteroaryl compounds such as 2-bromo-5-methylpyridine and 4-bromopyridine (Table 2, entries 12 and 13) reacted readily in the cyanation reaction to furnish the corresponding nitriles. We have also extended our studies to the normally less reactive aryl chlorides as the substrates under the same conditions. With increasing reaction time and increased catalyst amount, moderate yields are obtained (Table 2, entries 15–19).

In general, the cyanation reaction is clean. The pure products were obtained by a simple workup and column chromatography. Wide range of functionalities and heterocyclic moieties are tolerated in this procedure. In a scaled-up reaction at gram quantity of 4-nitroiodobenzene (2.5 g, 10 mmol), Pd NCs/C@

Fe_3O_4 (400 mg, 0.73 mol % of Pd) provided a high isolated yield (94%, TON = 128.4). These results indicated that Pd NCs/C@ Fe_3O_4 constitute a practical catalyst for the cyanation of aryl halides to produce aryl nitriles, amenable to gram scale operations also (Figure S7).

To gain an insight into structure catalytic activity relationship, we then turned our attention to study the catalytic performance of the cubical Pd NPs with mainly {100} surface facets, spherical Pd NPs with mixed surface facets, and commercially available Pd/C with undefined Pd structure. The enhanced catalytic activity of the {100} surface facets of cubical Pd NPs is clearly evident with the yield increasing from 58% for spherical Pd NPs to 99% for cubical Pd NPs. This reactivity increase is more than 1.5-fold and the TON increases 5.5-fold for Pd NCs compared to Pd NPs and Pd/C (Table 3).

Table 3. Effect of Shape in Cubical and Spherical Pd NPs on Cyanation Reaction^a

catalyst (mol)	yield (%) ^b	time (h)	TON
Pd NCs/C@ Fe_3O_4 (3.6×10^{-6})	99	10	135
Pd NPs/C@ Fe_3O_4 (3.1×10^{-6})	58	10	94
Pd/C (1.87×10^{-5})	95	10	25

^aReaction conditions: 4-iodonitrobenzene (0.5 mmol), $\text{K}_4[\text{Fe}(\text{CN})_6]$ (0.1 mmol); catalyst (20 mg, 0.73 mol % of Pd), Na_2CO_3 (0.2 mmol); temperature, 120 °C; DMF, 3 mL. ^bGC yield.

The origin of the enhanced reactivity observed with Pd NCs is generally attributed to the high density of low-coordinated atoms present at the surface of the catalyst. Though the cubic one has a much larger particle size (13 nm) than the spherical one (3–4 nm), Pd NCs show much higher activity than the Pd NPs with the same Pd metal content indicating that the shape effect is more important than the size effect in this case. This result, thus demonstrates that controlling the shape of the nanoparticles to expose more facets of high activity is indeed a very effective strategy to optimize the performance of the catalyst. It is relevant to note here that the leaching of Pd atoms from the surface of cubical Pd NPs is more when compared to spherical Pd NPs. TEM images of reused catalyst shows changes in their morphology (Figure 4). The presence of small nanoparticles in TEM images is due to the Pd residue deposited on the surface of C@ Fe_3O_4 after the reaction. These small particles are not present in the as-synthesized solution of the Pd NCs catalyst and so can be attributed to the leached Pd during the reaction.

The heterogeneity of the Pd NCs/C@ Fe_3O_4 catalyst was checked by carrying out a hot filtration test with *p*-nitroiodobenzene and $\text{K}_4[\text{Fe}(\text{CN})_6]$ as substrates, to find out whether Pd is leaching out from the solid catalyst to the solution or whether the catalyst is truly heterogeneous in nature. After continuing with the reaction under optimized conditions for about 7 h, the catalyst was filtered under hot conditions from the reaction mixture with 70% formation of 4-nitrobenzonitrile. After removal of the solid catalyst, the filtrate was then subjected to the reaction conditions for an additional 9 h, and no further yield of 4-nitrobenzonitrile was observed. The loss of catalytic activity can be attributed to the removal both of the parent nanocubes and the Pd clusters formed due to leaching. These results clearly demonstrate that Pd NCs/C@ Fe_3O_4 is truly heterogeneous in nature.

From an industrial perspective, one of the main advantages of using heterogeneous catalysts such as Pd NCs/C@ Fe_3O_4 is

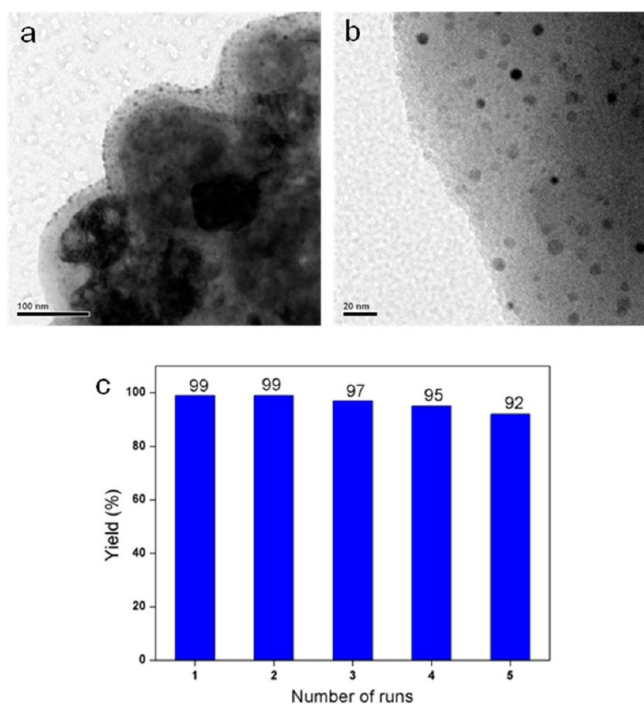


Figure 4. (a,b) TEM images of Pd NCs/C@Fe₃O₄ catalyst after 5 catalysis cycles and (c) reusability test using Pd NCs/C@Fe₃O₄ as catalyst for the cyanation of 4-nitroiodobenzene.

that they can be recovered and reused efficiently up to five consecutive runs (Figure 4c). After completion of the reaction, the solid catalyst was recovered by magnetic separation, extensively washed with EtOH, and dried at room temperature in a vacuum desiccator for 2 h. Only a marginal loss in the activity of the catalyst was observed up to five consecutive reactions. The TEM image of reused catalyst shows changes in structure (from cubical to spherical NPs), due to the enhanced leaching susceptibility of Pd {100} surface facets (Figure 4a,b). The powder XRD data of recycled Pd NCs/C@Fe₃O₄ (after the fifth cycle) clearly illustrate that the catalyst still remains as crystalline, and the average crystallite size estimated using Scherrer's equation is 8.2 nm. The particle size has decreased from 13 to 8.2 nm due to the increase in leaching susceptibility of Pd {100} surface facets (Figure S6).

On the basis of above results, a plausible reaction pathway for Pd catalyzed cyanation reaction involving a reaction mechanism in which Pd NCs on the surface of C@Fe₃O₄ NSs (Scheme 3) is proposed.^{29,34} In the first step, oxidative addition of aryl halides to Pd(0) leads to a Pd(II) species (A). In the second step, ligand exchange from the inner coordination sphere of K₄[Fe(CN)₆] to the Pd site of the catalyst (involving transmetalation) occurs to form the Pd(II) complex (B) and this is followed by reductive elimination to form aryl nitriles. Under our reaction system, the base and removed cyanide ion from K₄[Fe(CN)₆] is the primary source of Pd leaching; however, aryl halides also contributed to a lesser degree. Significantly, the catalytically active Pd species are generated by leaching of the surface atoms and this leaching mechanism is shape-sensitive. Preferential adsorption of molecular oxygen and cyanide ion on Pd {100} compared to Pd {111} surfaces induces greater Pd leaching when using Pd NCs, compared to Pd NPs.⁷⁵

Scheme 3. Proposed Mechanistic Pathway for the Cyanation of Arylhalides Using Pd NCs/C@Fe₃O₄

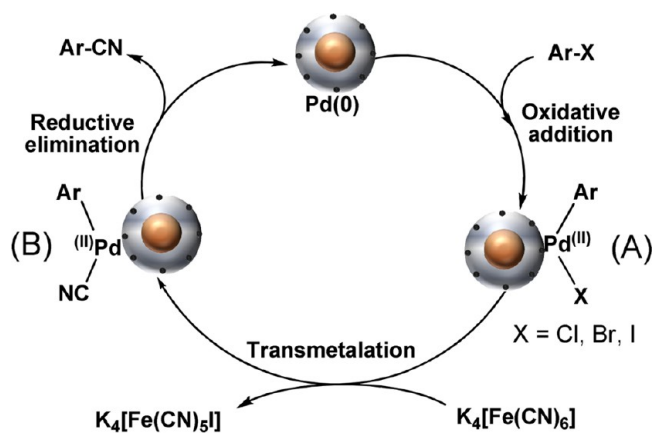


Table 4. Sheldon Test Carried out with Pd NCs/C@Fe₃O₄ Catalyzed Cyanation Reaction^a

catalyst	yield ^b (%)		
	7 h	(7 + 9) h	reused catalyst
Pd NCs/C@Fe ₃ O ₄	70	70	99

^aReaction conditions: 4-iodonitrobenzene (0.5 mmol), K₄[Fe(CN)₆] (0.1 mmol); catalyst (20 mg, 0.73 mol % of Pd), Na₂CO₃ (0.2 mmol); temperature, 120 °C; DMF, 3 mL. ^bGC yield.

Our catalytic system is also compared (Supporting Information, Table S1) with reported Pd containing catalytic systems for cyanation of aryl halides.^{30–53} The comparison table shows that most of the reported Pd catalysts are homogeneous in nature, use phosphine ligands, and possess high Pd content. However, the main disadvantage of using homogeneous catalysts is reusability. On the other hand, heterogeneous systems studied have more Pd content, but however display low catalytic efficiency, tedious synthetic procedures to prepare the catalysts, and Pd leaching during the reaction. In comparison our catalytic system is better in terms of facile synthesis of catalyst, higher catalytic efficiency with lower Pd content heterogeneous nature, reusability involving applying an external magnet, ligand free methodology, and applicability in gram scale synthesis.

CONCLUSIONS

In summary, we have developed highly efficient C@Fe₃O₄ magnetic core-shell nanospheres as a good support for palladium nanocubes with excessive {100} surface facets (Pd NCs/C@Fe₃O₄), and this is used as an heterogeneous catalyst with excellent catalytic activity in the cyanation of aryl iodides and bromides using K₄[Fe(CN)₆] as a green cyanating agent. A variety of aryl iodides and bromides were reacted in good to excellent yields to the corresponding nitriles. The marginal decrease in yield on reuse is attributed to the shape sensitivity of Pd{100} facets, which leads to a change in structure from cubic to spherical. It is anticipated that this approach may further expand the scope of investigations of various other active metal NPs and may aid the design of newer catalysts with possible uses to diverse substrates, excellent activity and tunable selectivity.

■ ASSOCIATED CONTENT

● Supporting Information

The Supporting Information is available free of charge on the ACS Publications website at DOI: 10.1021/acsami.5b08875.

UV-DRS, FT-IR spectra, and TGA analysis of synthesized Pd/C@Fe₃O₄ nanospheres. EDAX measurements for Pd in Pd/C@Fe₃O₄ nanospheres, powder XRD pattern of reused catalyst, details of gram scale synthesis, spectral data of aryl nitriles and ¹H, ¹³C NMR spectra (PDF)

■ AUTHOR INFORMATION

Corresponding Authors

*E-mail: jose.arlin@gmail.com.

*E-mail: pit12399@yahoo.com.

Notes

The authors declare no competing financial interest.

■ ACKNOWLEDGMENTS

B.S.K. gratefully acknowledges UGC, New Delhi, India, for Grant UGC-BSR-SRF. A.J.A. thanks DST, New Delhi, India, for the DST-INSPIRE Faculty Fellowship. K.P. appreciates financial support provided by CSIR. We jointly thank MKU-CIC for the HR-TEM facility under the UGC-UPE Programme.

■ REFERENCES

- (1) Malinsky, M. D.; Kelly, K. L.; Schatz, G. C.; Van Duyne, R. P. Nanosphere Lithography: Effect of Substrate on the Localized Surface Plasmon Resonance Spectrum of Silver Nanoparticles. *J. Phys. Chem. B* **2001**, *105*, 2343–2350.
- (2) Narayanan, R. Recent Advances in Noble Metal Nanocatalysts for Suzuki and Heck Cross-Coupling Reactions. *Molecules* **2010**, *15*, 2124–2138.
- (3) Link, S.; El-Sayed, M. A. Shape and Size Dependence of Radiative, Non-Radiative and Photothermal Properties of Gold Nanocrystals. *Int. Rev. Phys. Chem.* **2000**, *19*, 409–453.
- (4) Polshettiwar, V.; Varma, R. S. Green Chemistry by Nano-Catalysis. *Green Chem.* **2010**, *12*, 743–754.
- (5) Berger, C. E. H.; Beumer, T. A. M.; Kooyman, R. P. H.; Greve, J. Surface Plasmon Resonance Multisensing. *Anal. Chem.* **1998**, *70*, 703–706.
- (6) Brigger, I.; Dubernet, C.; Couvreur, P. Nanoparticles in Cancer Therapy and Diagnosis. *Adv. Drug Delivery Rev.* **2002**, *54*, 631–651.
- (7) Burda, C.; Chen, X. B.; Narayanan, R.; El-Sayed, M. A. Chemistry and Properties of Nanocrystals of Different Shapes. *Chem. Rev.* **2005**, *105*, 1025–1102.
- (8) Sun, H.; Ang, H. M.; Tade, M. O.; Wang, S. Co₃O₄ Nanocrystals with Predominantly Exposed Facets: Synthesis, Environmental and Energy Applications. *J. Mater. Chem. A* **2013**, *1*, 14427–14442.
- (9) Yin, A.-X.; Min, X.-Q.; Zhang, Y.-W.; Yan, C.-H. Shape-Selective Synthesis and Facet-Dependent Enhanced Electrocatalytic Activity and Durability of Monodisperse Sub-10 nm Pt-Pd Tetrahedrons and Cubes. *J. Am. Chem. Soc.* **2011**, *133*, 3816–3819.
- (10) Zhou, K.; Li, Y. Catalysis Based on Nanocrystals with Well-Defined Facets. *Angew. Chem., Int. Ed.* **2012**, *51*, 602–613.
- (11) Xie, X. W.; Li, Y.; Liu, Z. Q.; Haruta, M.; Shen, W. J. Low-Temperature Oxidation of CO Catalysed by Co₃O₄ Nanorods. *Nature* **2009**, *458*, 746–749.
- (12) Tsuji, J. *Palladium Reagents and Catalysts*; Wiley: Chichester, U.K., 1995.
- (13) Malleron, J.-L.; Fiaud, J.-C.; Legros, J.-Y. *Handbook of Palladium-Catalyzed Organic Reactions*; Academic Press: London, 2000.
- (14) Xiong, Y. J.; Xia, Y. N. Shape-Controlled Synthesis of Metal Nanostructures: The Case of Palladium. *Adv. Mater.* **2007**, *19*, 3385–3391.
- (15) Kleemann, A.; Engel, J.; Kutscher, B.; Reichert, D. *Pharmaceutical Substances: Syntheses, Patents, Applications*, 4th ed.; Georg Thieme: Stuttgart, Germany, 2001.
- (16) Sandmeyer, T. Ueber die Ersetzung der Amidgruppe durch Chlor in den aromatischen Substanzen. *Ber. Dtsch. Chem. Ges.* **1884**, *17*, 1633–1635.
- (17) Galli, C. Radical Reactions of Arenediazonium Ions: An Easy Entry into the Chemistry of the Aryl Radical. *Chem. Rev.* **1988**, *88*, 765–792.
- (18) Tsuji, J. *Transition Metal Reagents and Catalysts-Innovations in Organic Synthesis*; John Wiley & Sons: Chichester, U.K., 2000.
- (19) Brandsma, L.; Vasilevsky, S. F.; Verkruisje, H. D. *Application of Transition Metal Catalysts in Organic Synthesis*; Springer Verlag: Berlin, Heidelberg, Germany, 1999; p 149.
- (20) Heck, R. F. *Palladium Reagents in Organic Syntheses*; Academic Press: London, 1985.
- (21) Yu, H.; Richey, R. N.; Miller, W. D.; Xu, J.; May, S. A. Development of Pd/C-Catalyzed Cyanation of Aryl Halides. *J. Org. Chem.* **2011**, *76*, 665–668.
- (22) Cai, L.; Liu, X.; Tao, X.; Shen, D. Efficient Microwave-Assisted Cyanation of Aryl Bromide. *Synth. Commun.* **2004**, *34*, 1215–1221.
- (23) Sundermeier, M.; Mutyala, S.; Zapf, A.; Spannenberg, A.; Beller, M. A Convenient and Efficient Procedure for the Palladium-Catalyzed Cyanation of Aryl Halides Using Trimethylsilyl cyanide. *J. Organomet. Chem.* **2003**, *684*, 50–55.
- (24) Luo, F.-H.; Chu, C.-I.; Cheng, C.-H. Nitrile-Group Transfer from Solvents to Aryl Halides. Novel Carbon–Carbon Bond Formation and Cleavage Mediated by Palladium and Zinc Species. *Organometallics* **1998**, *17*, 1025–1030.
- (25) Sundermeier, M.; Zapf, A.; Beller, M. A Convenient Procedure for the Palladium Catalyzed Cyanation of Aryl Halides. *Angew. Chem., Int. Ed.* **2003**, *42*, 1661–1664.
- (26) Sato, N.; Yue, Q. An efficient synthesis of cyanoarenes and cyanoheteroarenes via lithiation followed by electrophilic cyanation. *Tetrahedron* **2003**, *59*, 5831–5836.
- (27) Anbarasan, P.; Schareina, T.; Beller, M. Recent Developments And Perspectives In Palladium-Catalyzed Cyanation of Aryl Halides: Synthesis of Benzonitriles. *Chem. Soc. Rev.* **2011**, *40*, 5049–5067.
- (28) Schareina, T.; Zapf, A.; Beller, M. Potassium hexacyanoferrate(II)-A New Cyanating Agent for the Palladium-Catalyzed Cyanation of Aryl Halides. *Chem. Commun.* **2004**, 1388–1389.
- (29) Schareina, A.; Zapf, A.; Beller, M. Improving Palladium-Catalyzed Cyanation of Aryl Halides: Development of a State-of-the-Art Methodology Using Potassium hexacyanoferrate(II) as Cyanating Agent. *J. Organomet. Chem.* **2004**, *689*, 4576–4583.
- (30) Weissman, S. A.; Zewge, D.; Chen, C. Ligand Free Palladium Catalyzed Cyanation of Aryl Halides. *J. Org. Chem.* **2005**, *70*, 1508–1510.
- (31) Velmathi, S.; Leadbeater, N. E. Palladium-Catalyzed Cyanation of Aryl Halides Using K₄[Fe(CN)₆] as Cyanide Source, Water as Solvent, and Microwave Heating. *Tetrahedron Lett.* **2008**, *49*, 4693–4694.
- (32) Grossman, O.; Gelman, D. Novel Trans-Spanned Palladium Complexes as Efficient Catalysts in Mild and Amine-Free Cyanation of Aryl Bromides under Air. *Org. Lett.* **2006**, *8*, 1189–1191.
- (33) Hajipour, A. R.; Karami, K.; Tavakoli, G.; Pirisedigh, A. An Efficient Palladium Catalytic System for Microwave Assisted Cyanation of Aryl Halides. *J. Organomet. Chem.* **2011**, *696*, 819–824.
- (34) Hajipour, A.-R.; Abrisham, F.; Tavakoli, G. Microwave-Enhanced Cyanation of Aryl Halides with a Dimeric ortho-Palladated Complex Catalyst. *Transition Met. Chem.* **2011**, *36*, 725–730.
- (35) Gerber, R.; Oberholzer, O.; Frech, C. M. Cyanation of Aryl Bromides with K₄[Fe(CN)₆] Catalyzed by Dichloro[bis{1-(dicyclohexylphosphanyl)piperidine}]palladium, a Molecular Source of Nanoparticles, and the Reactions Involved in the Catalyst-Deactivation Processes. *Chem. - Eur. J.* **2012**, *18*, 2978–2986.

- (36) Islam, M.; Mondal, P.; Tuhina, K.; Roy, A. S.; Mondal, S.; Hossain, D. Highly Efficient Recyclable Heterogeneous Palladium catalyst for C-C coupling, Amination and Cyanation reactions. *J. Organomet. Chem.* **2010**, *695*, 2284–2295.
- (37) Sawant, D. N.; Wagh, Y. S.; Tambade, P. J.; Bhatte, K. D.; Bhanage, B. M. Cyanides-Free Cyanation of Aryl Halides using Formamide. *Adv. Synth. Catal.* **2011**, *353*, 781–787.
- (38) Yu, H.; Richey, R. N.; Miller, W. D.; Xu, J.; May, S. A. Development of Pd/C-Catalyzed Cyanation of Aryl Halides. *J. Org. Chem.* **2011**, *76*, 665–668.
- (39) Yeung, P. Y.; Tsang, C. P.; Kwong, F. Y. Efficient Cyanation of Aryl Bromides with $K_4[Fe(CN)_6]$ Catalyzed by a Palladium-Indolylphosphine Complex. *Tetrahedron Lett.* **2011**, *52*, 7038–7041.
- (40) Zheng, S.; Yu, C.; Shen, Z. Ethyl Cyanoacetate: A New Cyanating Agent for the Palladium-Catalyzed Cyanation of Aryl Halides. *Org. Lett.* **2012**, *14*, 3644–3647.
- (41) Modak, A.; Mondal, J.; Bhaumik, A. Pd-grafted Periodic Mesoporous Organosilica: An Efficient Heterogeneous Catalyst for Hiyama and Sonogashira couplings, and Cyanation Reactions. *Green Chem.* **2012**, *14*, 2840–2855.
- (42) Zhang, G.-Y.; Yu, J.-T.; Hu, M.-L.; Cheng, J. Palladium-Catalyzed Cyanation of Aryl Halides with CuSCN. *J. Org. Chem.* **2013**, *78*, 2710–2714.
- (43) Guo, M.; Ge, J.; Zhu, Z.; Wu, X. Efficient Synthesis of Aromatic Nitriles via Cyanation of Aryl Bromides and $K_4[Fe(CN)_6]$ Catalyzed by a Palladium(II) Complex. *Lett. Org. Chem.* **2013**, *10*, 213–215.
- (44) Fu, L.; Li, X.; Zhu, Q.; Chen, S.; Kang, Y.; Guo, M. Efficient Cyanation of Aryl Halide with $K_4[Fe(CN)_6] \cdot 3H_2O$ Catalyzed by P-O Bidentate Chelate Palladium Complex Under Air. *Appl. Organomet. Chem.* **2014**, *28*, 699–701.
- (45) Sajadi, S. M.; Maham, M.; Mahmoud, S. A. $K_4[Fe(CN)_6]$ as non-toxic source of cyanide for the cyanation of aryl halides using Pd-Beta zeolite as a heterogeneous catalyst. *J. Chem. Res.* **2013**, *37*, 620–622.
- (46) Zhu, Y.-Z.; Cai, C. Pd/C: A Recyclable Catalyst for Cyanation of Aryl Halides with $K_4[Fe(CN)_6]$. *Synth. Commun.* **2007**, *37*, 3359–3366.
- (47) Chen, G.; Weng, J.; Zheng, Z.; Zhu, X.; Cai, Y.; Cai, J.; Wan, Y. Pd/C-Catalyzed Cyanation of Aryl Halides in Aqueous PEG. *Eur. J. Org. Chem.* **2008**, *2008*, 3524–3528.
- (48) Singh, A. S.; Shendage, S. S.; Nagarkar, J. M. Palladium supported on zinc ferrite: an efficient catalyst for ligand free C–C and C–O cross coupling reactions. *Tetrahedron Lett.* **2013**, *54*, 6319–6323.
- (49) Jiang, H.; Jiang, J.; Wei, H.; Cai, C. Heterogeneous Cyanation Reaction of Aryl Halides Catalyzed by a Reusable Palladium Schiff Base Complex in Water. *Catal. Lett.* **2013**, *143*, 1195–1199.
- (50) Niknam, K.; Deris, A.; Panahi, F. Silica-Functionalized N-Propylpiperazine for Immobilization of Palladium Nanoparticles as Efficient Heterogeneous Catalyst for Cyanation Reactions. *Chin. J. Catal.* **2013**, *34*, 718–722.
- (51) Chatterjee, T.; Dey, R.; Ranu, B. C. ZnO-Supported Pd Nanoparticle-Catalyzed Ligand- and Additive Free Cyanation of Unactivated Aryl Halides Using $K_4[Fe(CN)_6]$. *J. Org. Chem.* **2014**, *79*, 5875–5879.
- (52) Magdesieva, T. V.; Nikitin, O. M.; Zolotukhina, E. V.; Vorotyntsev, M. A. Palladium Nanoparticles–Polypyrrole Composite as an Efficient Catalyst for Cyanation of Aryl Halides. *Electrochim. Acta* **2014**, *122*, 289–295.
- (53) Karimi, B.; Zamani, A.; Mansouri, F. Activity Enhancement in Cyanation of Aryl Halides through Confinement of Ionic Liquid in the Nanospaces of SBA-15 Supported Pd Complex. *RSC Adv.* **2014**, *4*, 57639–57645.
- (54) Marck, G.; Villiger, A.; Buchecker, R. Aryl Couplings with Heterogeneous Palladium Catalysts. *Tetrahedron Lett.* **1994**, *35*, 3277–3280.
- (55) LeBlond, C. R.; Andrews, A. T.; Sun, Y.; Sowa, J. R. Activation of Aryl Chlorides for Suzuki Cross-Coupling by Ligandless, Heterogeneous Palladium. *Org. Lett.* **2001**, *3*, 1555–1557.
- (56) Choudary, B. M.; Madhi, S.; Chowdari, N. S.; Kantam, M. L.; Sreedhar, B. Layered Double Hydroxide Supported Nanopalladium Catalyst for Heck-, Suzuki-, Sonogashira-, and Stille-Type Coupling Reactions of Chloroarenes. *J. Am. Chem. Soc.* **2002**, *124*, 14127–14136.
- (57) Gauthier, D.; Baillargeon, P.; Drouin, M.; Dory, Y. L. Self-Assembly of Cyclic Peptides into Nanotubes and Then into Highly Anisotropic Crystalline Materials. *Angew. Chem., Int. Ed.* **2001**, *40*, 4635–4638.
- (58) Akiyama, R.; Kobayashi, S. Microencapsulated Palladium Catalysts: Allylic Substitution and Suzuki Coupling Using a Recoverable and Reusable Polymer-Supported Palladium Catalyst. *Angew. Chem., Int. Ed.* **2001**, *40*, 3469–3471.
- (59) Puthiaraj, P.; Pitchumani, K. Palladium Nanoparticles Supported on Triazine Functionalised Mesoporous Covalent Organic Polymers as Efficient Catalysts for Mizoroki–Heck Cross Coupling Reaction. *Green Chem.* **2014**, *16*, 4223–4233.
- (60) Affrose, A.; Suresh, P.; Azath, I. A.; Pitchumani, K. Palladium Nanoparticles Embedded on Thioureamodified Chitosan: A Green and Sustainable Heterogeneous Catalyst for the Suzuki Reaction in Water. *RSC Adv.* **2015**, *5*, 27533–27539.
- (61) Amali, A. J.; Rana, R. K. Stabilisation of Pd(0) on Surface Functionalised Fe_3O_4 Nanoparticles: Magnetically Recoverable and Stable Recyclable Catalyst for Hydrogenation and Suzuki–Miyaura Reactions. *Green Chem.* **2009**, *11*, 1781–1786.
- (62) Kainz, Q. M.; Linhardt, R.; Grass, R. N.; Vile, G.; Perez-Ramirez, J.; Stark, W. J.; Reiser, O. Palladium Nanoparticles Supported on Magnetic Carbon Coated Cobalt Nanobeads: Highly Active and Recyclable Catalysts for Alkene Hydrogenation. *Adv. Funct. Mater.* **2014**, *24*, 2020–2027.
- (63) Lu, A.-H.; Schmidt, W.; Matoussevitch, N.; Boïnemann, H.; Spliethoff, B.; Tesche, B.; Bill, E.; Kiefer, W.; Schuth, F. Nano-engineering of a Magnetically Separable Hydrogenation Catalyst. *Angew. Chem., Int. Ed.* **2004**, *43*, 4403–4306.
- (64) Jin, M.; Liu, H.; Zhang, H.; Xie, Z.; Liu, J.; Xia, Y. Synthesis of Pd Nanocrystals Enclosed by {100} Facets and with Sizes < 10 nm for Application in CO Oxidation. *Nano Res.* **2011**, *4*, 83–91.
- (65) Zhang, Y.; Shu, H.; Chang, G.; Ji, K.; Oyama, M.; Liu, X.; He, Y. Facile Synthesis of Palladium–Graphene Nanocomposites and their Catalysis for Electro-Oxidation of Methanol and Ethanol. *Electrochim. Acta* **2013**, *109*, 570–576.
- (66) Wang, H.-Q.; Wei, X.; Wang, K.-X.; Chen, J.-S. Controlled Synthesis of Magnetic Pd/ Fe_3O_4 Spheres via an Ethylenediamine Assisted Route. *Dalton Trans.* **2012**, *41*, 3204–3208.
- (67) Zhang, Z.; Duan, H.; Li, S.; Lin, Y. Assembly of Magnetic Nanospheres into One-Dimensional Nanostructured Carbon Hybrid Materials. *Langmuir* **2010**, *26*, 6676–6680.
- (68) Zhu, M.; Diao, G. Magnetically Recyclable Pd Nanoparticles Immobilized on Magnetic Fe_3O_4 @C Nanocomposites: Preparation, Characterization, and Their Catalytic Activity toward Suzuki and Heck Coupling Reactions. *J. Phys. Chem. C* **2011**, *115*, 24743–24749.
- (69) Hao, D.; Xue-Zhao, S.; Cheng-Min, S.; Chao, H.; Zhi-Chuan, X.; Chen, L.; Yuan, T.; Deng-Ke, W.; Hong-Jun, G. Synthesis of Monodisperse Palladium Nanocubes and their Catalytic Activity for Methanol Electrooxidation. *Chin. Phys. B* **2010**, *19*, 106104–5.
- (70) Kulkarni, S. A.; Sawadh, P. S.; Palei, P. K. Synthesis and Characterization of Superparamagnetic Fe_3O_4 @ SiO_2 Nanoparticles. *J. Korean Chem. Soc.* **2014**, *58*, 100–104.
- (71) Wagner, C. D.; Riggs, W. M.; Davis, L. E.; Moulder, J. F. *Handbook of X Ray Photoelectron Spectroscopy*; Muilenberg, G. E., Ed.; Perkin Elmer Corporation: Eden Prairie, MN, 1978.
- (72) Beletskaya, I. P.; Selivanova, A. V.; Tyurin, V. S.; Matveev, V. V.; Khokhlov, A. R. Palladium nanoparticles stabilized by a copolymer of N-vinylimidazole with N-vinylcaprolactam as efficient recyclable catalyst of aromatic cyanation. *Russ. J. Org. Chem.* **2010**, *46*, 157–161.
- (73) Schareina, T.; Jackstell, R.; Schulz, T.; Zapf, A.; Cotte, A.; Gotta, M.; Beller, M. Increasing the Scope of Palladium-Catalyzed Cyanations of Aryl Chlorides. *Adv. Synth. Catal.* **2009**, *351*, 643–648.

(74) Zanon, J.; Klapars, A.; Buchwald, S. L. Copper-Catalyzed Domino Halide Exchange-Cyanation of Aryl Bromides. *J. Am. Chem. Soc.* **2003**, *125*, 2890–2891.

(75) Collins, G.; Schmidt, M.; O'Dwyer, C.; McGlacken, G.; Holmes, J. D. Enhanced Catalytic Activity of High-Index Faceted Palladium Nanoparticles in Suzuki-Miyaura Coupling Due to Efficient Leaching Mechanism. *ACS Catal.* **2014**, *4*, 3105–3111.